Electronic Supplementary Material (ESI) for Physical Chemistry Chemical Physics.

Synthesis of branched Pd nanocrystals with tunable structures, their growth mechanism, and enhanced electrocatalytic properties

Xueli Guo and Yiwei Tan*

State Key Laboratory of Materials-Oriented Chemical Engineering, School of Chemistry and Chemical Engineering, Nanjing Tech University, Nanjing 210009, China, Email: ytan@njtech.edu.cn, Tel: +86-25-83172267

Experimental section

Materials: All reagents were commercially available and used as received. $PdCl_2$ (Pd >59%), $CuBr_2$ (99%), NaBr (>99%), hydrochloric acid (36.5–38% HCl), and hexadecyltrimethylammonium bromide (CTAB, >99%) were commercially available from Sinopharm Chemical Reagent Co., Ltd.. L-Ascorbic acid (L-AA, >99%) and hexadecyltrimethylammonium chloride (CTAC) were purchased from Alfa Aesar. An aqueous solution of 10 mM H_2PdCl_4 was prepared by dissolving 0.089 g (0.5 mmol) of $PdCl_2$ in 50 mL of an aqueous solution of 0.02 M HCl at 60 °C under vigorous magnetic stirring and then used as the stock solution for the synthesis of various branched Pd nanocrystals. Ultrapure water (18.2 MΩ) produced with a Milli-Q purification system was used in all syntheses and electrochemical measurements.

Electrochemical measurements: Electrochemical measurements were performed using a glassy carbon (GC) electrode (Pine Research Instrumentation, 5 mm in diameter, 0.196 cm^2) connected to a CHI 660D electrochemical analyzer (CH Instruments, Chen-Hua Co., Shanghai, China) in a three-electrode glass cell at room temperature. A Ag/AgCl or Hg/HgO was used as the reference electrode in acid or alkaline medium, respectively. A Pt wire was used as the counter electrode. The GC disk electrodes were polished using 0.05 μm alumina slurries and then were thoroughly rinsed with deionized water and dried under ambient conditions before acting as the substrate for the supported Pt/C (Johnson Matthey, 20 wt% of 3.2 nm Pt nanoparticles on Vulcan XC-72 carbon support), Pd/C (Johnson Matthey, 20 wt% of ~4 nm Pd nanoparticles on Vulcan XC-72 carbon black), or branched Pd catalysts. All potentials were applied against the reference electrodes and were converted into the reversible hydrogen electrode (RHE) in terms of the Nernst equation ($V_{RHE} = V_{Ag/AgCl\ or\ Hg/HgO} + E_{Ag/AgCl\ or\ Hg/HgO} + 0.059$ pH, where V_{RHE} and $V_{Ag/AgCl\ or\ Hg/HgO}$ are the applied potentials versus RHE and Ag/AgCl or Hg/HgO reference electrode, respectively. $E_{Ag/AgCl\ or\ Hg/HgO}$ is the reference electrode potential versus the standard hydrogen electrode).

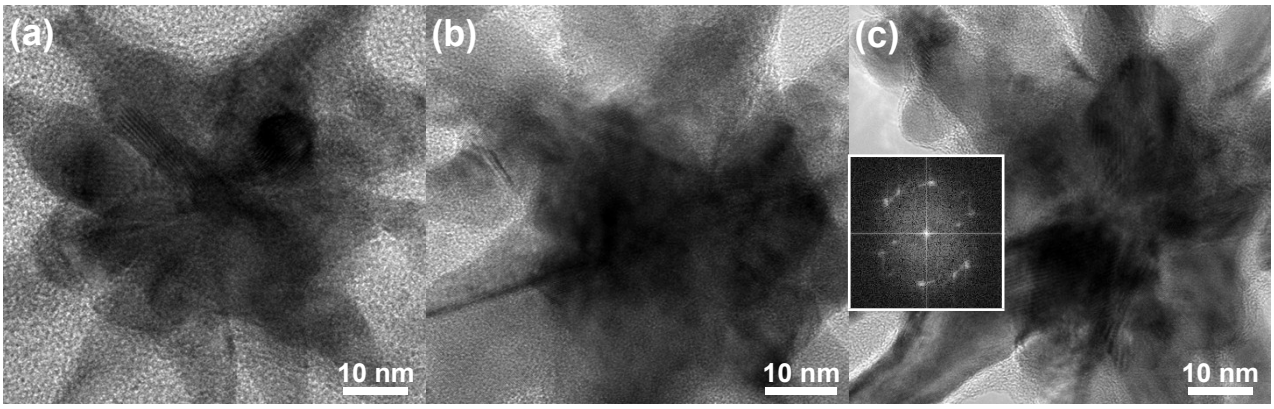

Figure S1. HRTEM images show a zoom-in view of the central core domain of a branched Pd NC from (a) sample 2, (b) sample 3, and (c) sample 4. The inset shows the corresponding fast Fourier transform (FFT) pattern.

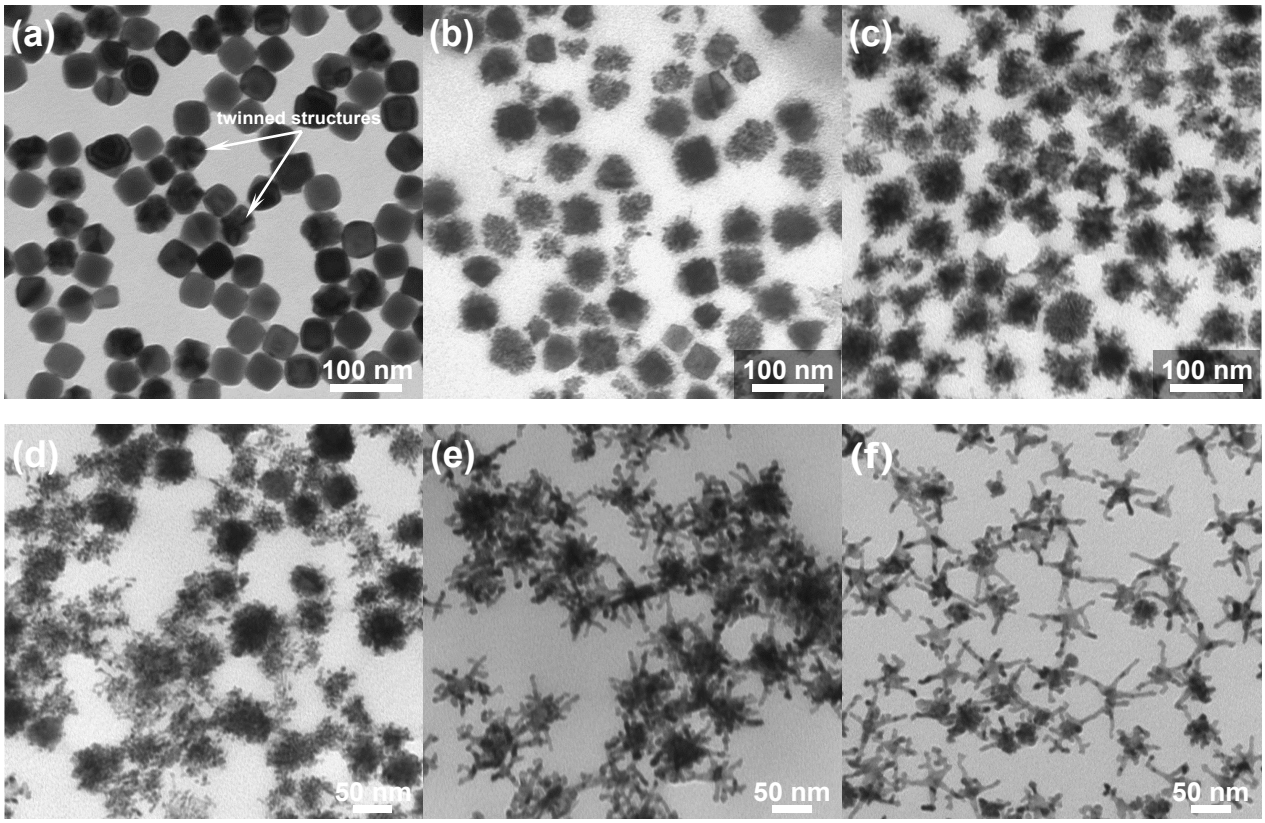

Figure S2. TEM images showing the temporal structural evolution of the Pd NCs (sample 2): (a) 7.5 min, (b) 10 min, (c) 30 min, (d) 40 min, (e) 50 min, and (f) 60 min.

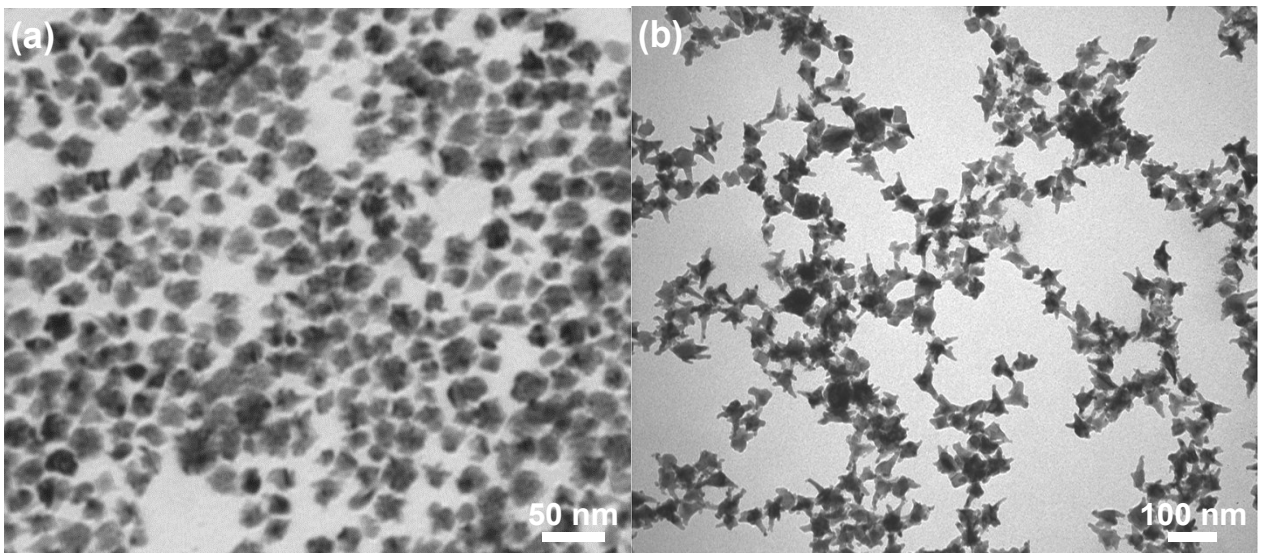

Figure S3. TEM images of the Pd nanoparticles synthesized (a) when CTAB is replaced by CTAC and (b) in the absence of Cu^{2+} ions. Other experimental conditions are identical to those for the synthesis of sample 3.

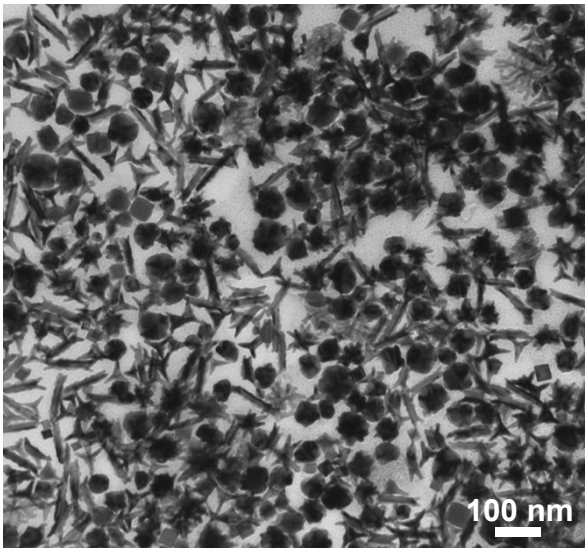

Figure S4. TEM image of the Pd nanoparticles synthesized by incubating the mixture of CTAB, Cu ions, and L-AA for 20 min prior to the addition of H_2PdCl_4 (1.0 mM in the final solution).

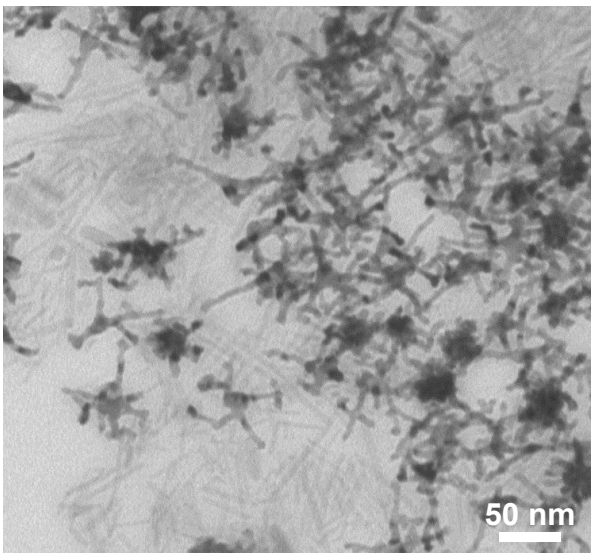

Figure S5. TEM image of sample 2 showing the rod-like micelles together with the branched Pd NCs on the TEM copper grids.

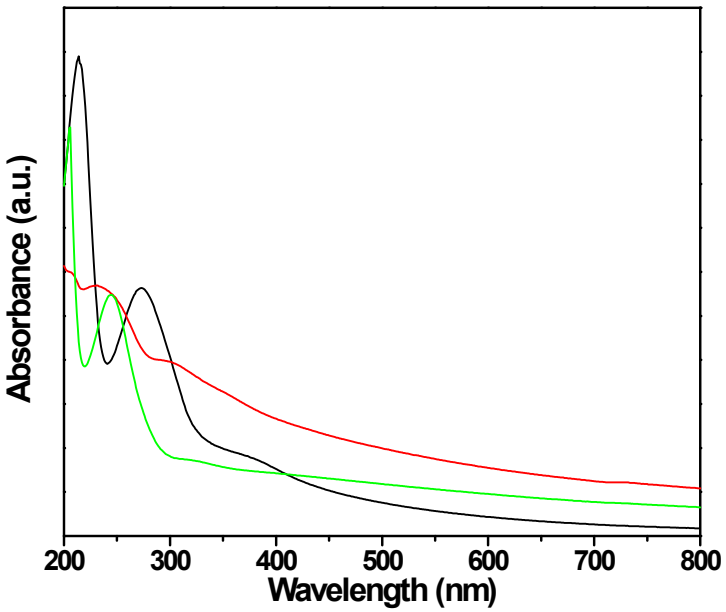

Figure S6. UV-vis absorption spectra of the $[CTA^+]_2[PdCl_4^{2-}]$ complex formed by mixing two equivalent CTAB and one H_2PdCl_4 (black plot), an aqueous solution of CTAB (10 mM), CuBr (5 mM), and NaBr (5 mM) (red plot), and a solution of CTAB (10 mM), $CuBr_2$ (5 mM), and L-AA (10 mM) (green plot).

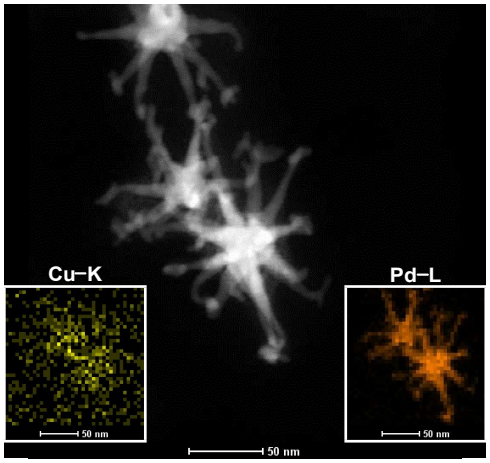

Figure S7. A representative high-angle annular dark-field scanning TEM (HAADF-STEM) image of the branched Pd nanocrystals obtained from sample 2. The insets show the corresponding elemental mapping images. As can be seen, the presence of Cu is dubious because of a very low signal-to-noise ratio caused by its trace content.